Applied Geochemistry 94 (2018) 11–20

Contents lists available at ScienceDirect

Applied Geochemistry

journal homepage: www.elsevier.com/locate/apgeochem

Erosion behaviour of raw bentonites under compacted and confined conditions: Relevance of smectite content and clay/water interactions

Ursula Alonso*, Tiziana Missana, Ana María Fernández, Miguel García-Gutiérrez

CIEMAT, Department of Environment, Avenida Complutense 40, 28040 Madrid, Spain

ARTICLE INFO

Keywords:
Bentonite
Erosion
Smectite
Colloids
Radioactive waste
Clay/water interactions

ABSTRACT

The quantification of colloid erosion from compacted bentonite barrier, in a high-level waste repository, is considered especially relevant because erosion may compromise its performance and because eroded colloids may contribute to radionuclide transport.

The erosion behaviour of different raw bentonites, compacted at high density, was analysed in a confined system under favourable chemical conditions. A complete physical and geochemical characterisation of clays was carried out to overall relate clay physico-chemical characteristics and structure to their erosion behaviour.

The mass eroded under compacted and confined conditions were in all cases lower than those obtained under free-dispersed conditions; indicating that compacted and confined conditions were limiting erosion. Maximum erosion was below a 1% of the initial mass.

Results clearly showed that clay erosion under compacted state was hindered for those bentonites with high content of bivalent cations in exchangeable positions ((Ca + Na) > 90%), low smectite content (Sm. < 70 wt %) and high tetrahedral charge ($|\tau| > 0.1$ *e*/h.u.c.). In addition, it was demonstrated that, at high solid to liquid ratios, dissolution of salts present in the clay and cation exchange reactions decrease the extent of erosion.

1. Introduction

Compacted bentonite is an engineered barrier considered in high-level radioactive waste (HLRW) repositories to confine the waste (Chapman, 2006; Pusch, 2008; Sellin and Leupin, 2013). It is widely accepted that clay selected by this scope should have high smectite content, to develop sufficient swelling pressure, to provide low hydraulic conductivity and to hinder radionuclide migration, altogether contributing to repository safety (Kaufhold and Dohrmann, 2016; Sellin and Leupin, 2013). The characteristics that make smectite appropriate are related to its layered structure where two tetrahedral (τ) sheets sandwich and octahedral (O) sheet conforming a TOT structure type 2:1, which is balanced by an interlayer of hydrated cations (e.g. Odom, 1984).

Amongst the main processes that may compromise the bentonite performance, erosion and colloid formation are considered of concern (Missana et al., 2011; Sellin and Leupin, 2013). Erosion is defined as the removal of surface material and its transportation by a natural agent, in this context flowing water, which can favour both mechanical and physical weathering. Bentonite erosion causes mass loss which directly affects the barrier integrity and performance. In addition, eroded colloids (particles in suspension with diameters < 1 μm) may contribute to radionuclide transport (Missana et al., 2008; Ryan and Elimelech, 1996; Schaefer et al., 2012).

Clay erosion has been widely studied in the field of soil resistance to water and irrigation (Grissinger, 1966) and many relevant issues can be extracted from this field, as the relevance of mineral composition, clay content, calcium/magnesium ratios or free oxides content (Bütak, 2005; Morgan, 2004). However, the particular conditions of a bentonite barrier in a HLRW repository, where the clay is compacted at high density and confined by the repository host rock (Chapman, 2006; Pusch, 2008; Sellin and Leupin, 2013), may influence its erosion behaviour.

In order for erosion to occur, the bentonite barrier must be saturated with the groundwater coming from the repository host rock. The processes that come up during clay hydration are well described (e.g. Gailhanou et al., 2017). Due to hydration, clay individual layers can be separated, causing delamination or large clay aggregates can be decompose in smaller particles, by exfoliation. Also, when compacted bentonite is hydrated, swelling is favoured (Norrish, 1954) and the clay will intrude in available pore spaces and micro-fractures. If a local hydraulic gradient does not exist, diffusion will be the driving force for colloid releases (Kallay et al., 1987), and free dispersion may primarily promote bentonite erosion and colloid formation.

* Corresponding author.
E-mail address: ursula.alonso@ciemat.es (U. Alonso).

https://doi.org/10.1016/j.apgeochem.2018.04.012
Received 24 December 2017; Received in revised form 24 April 2018; Accepted 25 April 2018
Available online 01 May 2018
0883-2927/

Mechanical forces, like those produced by water advective flow may additionally favour clay erosion and colloid detachment. Erosion under flow conditions depends on flow velocity, water chemical composition and fracture conditions (Birgersson et al., 2009; Missana et al., 2011; Pusch, 1999; Schatz et al., 2013).

To assess the magnitude of bentonite erosion, and to identify the mechanisms and geochemical conditions that favour it in a HLRW repository, different experimental approaches have been proposed with dispersed or compacted clay, accounting for stagnant and flow conditions, both in open or closed systems (Albarran et al., 2014; Alonso et al., 2007; Baik et al., 2007; Bessho and Degueldre, 2009; Birgersson et al., 2009; Degueldre and Benedicto, 2012; Garcia-Garcia et al., 2009; Kaufhold and Dohrmann, 2008; Liu and Neretnieks, 2006; Missana et al., 2003, 2011; Pusch, 1999; Schatz et al., 2013; Seher et al., 2009).

Conceptual models have been also developed to describe particle detachment by diffusion (Kallay et al., 1987), or swelling and detachment promoted by advective flow (Liu and Neretnieks, 2006; Liu, 2010; Liu et al., 2009; Neretnieks et al., 2009). These models sometimes apply to simplified systems: flat surfaces, Na-homoionic clays and low ionic strength groundwater. To date, uncertainties are still associated to bentonite erosion and colloid formation processes, under real repository conditions, preventing the precise quantification of erosion and colloid formation at the bentonite/host rock interface.

Clay dispersion in water has been analysed in different groundwaters (Birgersson et al., 2011; Garcia-Garcia et al., 2009; Kaufhold and Dohrmann, 2008; Luckham and Rossi, 1999; Norrish, 1954; Pertsov, 2005; Pusch, 1999); it occurs when attractive forces between the clay particles are overcome. It is well accepted that groundwater with low ionic strength and low content of divalent cations promotes peptisation (deflocculation), and favour the separation of individual smectite layers, giving to the clay/water system a sol character and favouring spontaneous colloid formation (Birgersson et al., 2011; Sen and Khilar, 2006). On the contrary, in groundwaters whose ionic strength is above the minimum concentration to cause flocculation, smectite forms a coherent gel inhibiting particles release and restricting colloid stability (Luckham and Rossi, 1999; Missana et al., 2003, 2018a).

In a recent study (Missana et al., Submitted), the dispersion of smectite clays was analysed by adding one gram of clay to one litre of deionised water. After centrifuging the sample, the mass, surface charge and size of dispersed colloids were obtained, under the most favourable conditions in terms of low ionic strength water. The intrinsic characteristics of colloids dispersed from different smectite clays were related to the main physico-chemical and structural properties of the bulk smectite (Missana et al., Submitted). Maximum colloid dispersion was measured for Na-homoionic smectites, while significant lower amounts were dispersed from Ca-smectites. It was found that the governing clay characteristics that promote colloid dispersion are the smectite content, the Na predominance as interlayer cation, and the layer charge and the charge distribution between the octahedral (O) and tetrahedral (τ) smectite layers.

Bentonite erosion and colloid dispersion may be different under compacted and confined conditions because, the interlayer space is in the nanometre scale, affecting the electrical interactions (overlapping of electrical double layers). Moreover, the high ion concentration of the clay porewater (Bradbury and Baeyens, 2009; Fernández et al., 2004; Karnland et al., 2011; Wersin et al., 2016), may affect the water conditions at equilibrium, especially at high solid to liquid ratios.

The aim of this study is to analyse which physico-chemical factors are playing a major role in the erosion and colloid formation under compacted and confined conditions. An experimental set-up previously developed to these purposes was selected (Albarran et al., 2014; Alonso et al., 2007). In previous experiments, the effect of compaction density, water chemistry and dominant exchange cation were analysed with a Ca-Mg bentonite (FEBEX, Huertas et al., 2000). It was demonstrated that higher erosion was promoted at higher compaction densities (Alonso et al., 2007), with homoionic Na-bentonite and in low ionic strength waters (Albarran et al., 2014).

The present study was focused on relating erosion results to the inherent physico-chemical properties of clay minerals, and also to evaluate the relevance of the water chemistry at equilibrium, two aspects that were not previously analysed. Experimental conditions were selected to account for the most favourable conditions for erosion: high compaction density and deionised water (Albarran et al., 2014; Alonso et al., 2007).

To analyse the relevance of clay physico-chemical characteristics on erosion, fourteen different clays were selected. They are mainly raw bentonites from different origin and reference clays, from the Minerals Society Source Clays Repository, representative of relevant clay minerals from the smectite group (montmorillonite, beidellite, nontronite and saponite). Selected clays cover a wide range of physico - chemical and structural conditions. They were fully characterised (Fernández et al., 2017a) to facilitate their classification from the point of view of their erodibility in a HLRW repository.

The bentonite erosion results obtained in compacted and confined conditions were compared to those determined for the same clays under free dispersed conditions, were maximum erosion is achieved (Missana et al., Submitted). With this comparison we aimed to highlight additional aspects to be accounted for quantifying bentonite erosion in a repository, like the chemical equilibrium between the clay and the groundwater.

The water chemistry evolves when in contact with the clay, because soluble salts and minerals dissolve and because cation exchange processes take place. This chemical evolution is limited under low solid to liquid ratio, but clay/water chemical interactions may play a major role on erosion processes under repository conditions.

2. Materials and methods

2.1. Clay minerals

Fourteen clayey materials were selected for the study. They are mainly raw bentonites studied in the frame of radioactive waste management research programmes and also clays from the Minerals Society Source Clays Repository, which are representative of relevant clay minerals from the smectite group. Selected clay minerals, their origin and references where more information about the clays can be obtained are included in Table 1.

All selected clay minerals lay within the smectite group (Guggenheim et al., 2006). Smectite is a planar hydrous phyllosilicate, with a layered structure, where two tetrahedral (τ) sheets sandwich and octahedral (O) sheet (TOT structure type 2:1). When the tetrahedral and octahedral sheets are joined in a layer, the resulting structure is electrically charged which is balanced by a cation interlayer sheet. Smectite clay minerals possess a negative permanent layer charge which arises from cation substitutions in the phyllosilicate sheets, conferring smectites assorted structure and chemical composition.

Selected clays were characterised to evaluate their main physico-chemical and structural characteristics. Full details on clay characterisation can be found in (Fernández et al., 2017a). Major and minor minerals, clay minerals content, and the main structural features that allow smectite classification (Emmerich et al., 2009; Guggenheim et al., 2006) were determined: dioctahedral or trioctahedral nature, clay mineral layer charge, charge distribution between tetrahedral (T) and octahedral (O) sheets, cation distribution within the octahedral sheet and inside the interlayer. It is noteworthy that all these physico-chemical properties were determined on the same samples used for erosion experiments, applying to all the same methodology, to facilitate comparison and generalisation of smectite erosion process. Obtained values are comparable to those reported in the literature (i.e., MX-80 or IBECO, in Karnland (2010)).

Table 2 presents the main characteristics of the analysed clays. All clays are 2:1 phyllosilicates with a layer charge between 0.25*e* and

Table 1
Selected clays, type, origin and reference, initial experimental conditions: weighted masses (g) and initial water content (w.c in %).

Clay	Type	Origin/location	References	Weighted mass (g)	w.c (%)
Nanocor®	2:1 Na-smectite	Commercial, China	http://www.nanocor.com/	4.813	16.00
MSU	2:1 Na- smectite	Khakassia deposit, Russia	Sabodina et al., 2006	4.398	6.84
FEBEX	2:1 Ca-Mg smectite	Cortijo de Archidona, Almeria, Spain	Huertas et al., 2000	4.756	13.56
MX-80	2:1 Na smectite	Wyoming, USA	Müller-Vonmoss and Kahr, 1983	4.387	6.57
MILOS-IBECO	2:1 Ca-Mg smectite	Milos island, Greece (sample IBECO RWC 16)	Koch, 2002; Koch, 2008	4.739	12.92
Rokle S65 Sabenil	2:1 Na smectite (fully activated)	Rokle deposit, Czech Republic	Konta, 1986	4.514	8.56
Rokle B75	2:1 Na-Mg Sm (partially Na-activated)	Rokle deposit, Czech Republic	Konta, 1986	4.418	6.84
Ypresian YC-Doel-40	2:1 Na- smectite	Doel nuclear zone in Antwerpen, Belgium (378.78–379.58 m depth)	Nguyen et al., 2014	4.282	4.05
Ypresian YC-Kallo-38	2:1 Na-smectite	Kallo town in Beveren, Belgium (324.89–325.84 m depth)	Marcke and Laenen, 2005	4.301	4.48
SBId-1	2:1 Ca beidellite	Idaho, USA (Clay Mineral Society)	Post et al., 1997	4.498	8.52
NAu-1	2:1 Ca-Mg nontronite Fe-rich	Uley Graphite Mine, Australia (Clay Mineral Society)	Keeling et al., 2000	4.743	12.80
SAz-2 - Cheto	2:1 Ca-smectite	Arizona, USA (Clay Mineral Society)	Jaynes and Bigham, 1987	4.948	17.42
MCA-C	2:1 Mg saponite	Cerro del Aguila, Spain	Cuevas et al., 1993; Pusch et al., 1996	4.615	10.93
B64	2:1 Mg saponite	Grevena, Macedonia	Kastridis et al., 2003; Kaufhold et al., In Prep	4.633	12.54

0.60*e* per $O_{10}(OH)_2$ half unit cell (h.u.c), where *e* is the electron charge ($1.6{\cdot}10^{-19}$ C). Most of them are dioctahedral smectites, except for the two saponites (MCA-C and B64) which are trioctahedral. Dioctahedral smectites with low or null tetrahedral charge can be defined as montmorillonites, where layer charge in the octahedral sheet is mainly generated by substitution of Al^{3+} by Mg^{2+}. In contrast, beidellite is the end-member with mainly tetrahedral charge and low octahedral charge. Nontronite is characterised by a large Fe content in the octahedral sheet, and it is regarded as the third end-member of dioctahedral smectites.

At higher solid to liquid ratio, the dissolution of soluble salts present in the clay, mainly halite, gypsum and calcite, will establish a chemical equilibrium that may be relevant for erosion process under studied conditions. Table 3 presents the anion inventory (Cl^- and SO_4^{2-} content in mmol/100 g of clay) measured for studied clays (Fernández et al., 2017a). The clays with higher salt inventory are NANOCOR® and MSU.

Table 3
Anion inventory in studied clays (Fernández et al., 2017a).

Clay	Cl	SO_4
	mmol/100 g	mmol/100 g
NANOCOR®	4.40	10.68
MSU	2.06	1.82
FEBEX	3.01	0.78
MX-80	1.36	3.26
MILOS-IBECO	1.82	1.35
Rokle-B75	1.22	0.11
Rokle-S65	1.27	0.07
YC-Doel-40	5.05	0.66
YC-Kallo-38	1.62	1.31
SBdI-1 (beidellite)	1.29	0.15
NAu-1 (nontronite)	2.87	0.08
SAz-2 - Cheto	1.32	0.00
MCA-C (saponite)	1.56	0.09
B64 (saponite)*	1.50	0.00

2.2. Experimental set-up: erosion cell and analyses

Fig. 1 shows the experimental set-up used to quantify bentonite erosion and colloid formation from bentonite under compacted and confined conditions. The selected dry density was 1.65 g cm^{-3}, a value in the upper range of densities considered by different national concepts of HLRW repositories (Sellin and Leupin, 2013).

Table 2
Physico-chemical and structural characteristics determined for studied clays (Fernández et al., 2017a). *B64 data from (Kastridis et al., 2003).

Clay	Smectite	Na	Ca + Mg	Tetrahedral Charge (*e*/h.u.c)	Octahedral Charge (*e*/h.u.c)	Layer charge (*e*/h.u.c)	Charge density (C/m^2)
	(wt. %)	(%)	(%)				
Nanocor®	98	93.45	2.51	−0.04	−0.34	−0.38	0.13
MSU	79	90.24	4.46	−0.14	−0.21	−0.35	0.12
FEBEX	94	27.77	66.43	−0.07	−0.31	−0.38	0.13
MX-80	89	68.32	26.27	−0.08	−0.2	−0.28	0.10
MILOS-IBECO	88	26.30	68.97	−0.04	−0.29	−0.33	0.11
Rokle S65 Sabenil	78	76.93	16.66	−0.26	−0.11	−0.37	0.13
Rokle B75	78	55.67	34.64	−0.29	−0.11	−0.40	0.14
YC-Doel-40	26	47.61	34.09	−0.14	−0.24	−0.38	0.13
YC-Kallo-38	30	56.86	30.48	−0.14	−0.26	−0.40	0.14
SBId-1	78	0.73	92.01	−0.26	−0.06	−0.32	0.11
NAu-1	90	3.78	91.32	−0.32	−0.05	−0.37	0.12
SAz-2 - Cheto	98	0.44	94.64	0	−0.5	−0.50	0.17
MCA-C	78	4.16	87.95	−0.25	−0.15	−0.40	0.13
B64	65	0.33	92.29	−0.13	−0.38	−0.51	0.17

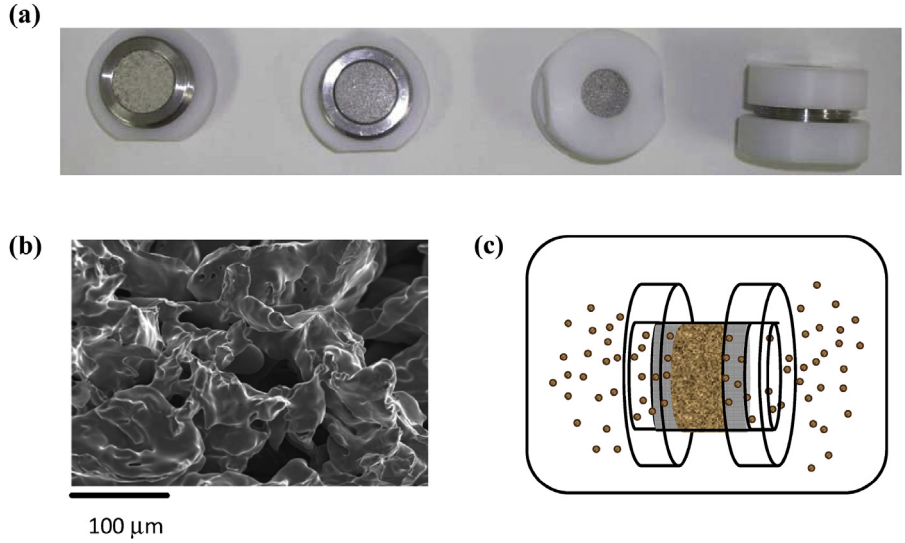

Fig. 1. (a) Set-up used to analyse bentonite erosion under compacted and confined conditions; (b) SEM image of stainless steel filter surface with 100 µm pore size; (c) Outline of erosion process and colloid formation in selected set-up.

In the set-up, the compacted bentonite pellet (approximately 4–4.5 grams, depending on clay humidity) was placed in a stainless-steel cylinder and it is sandwiched between two sintered stainless-steel filters. Table 1 presents the weighted masses and the initial water content (w.c. in %) of studied clays. The filters have 20 mm diameter and 3 mm thickness and a pore size of 100 µm, as can be appreciated in the SEM image presented in Fig. 1b. A porosity of 38% was estimated from the dimensions and mass of the filter.

The cell is closed by two open Delrin grids that guarantee clay confinement but allowing the release of eroded particles through both filters (Fig. 1c) being the total surface available for particle releases of 3.54 cm^2.

To promote clay erosion, the cell is immersed in 200 mL of deionised water (DW), to account for the most favourable conditions for erosion (low ionic strength and absence of divalent cations) (Missana et al., 2011). All experiments were carried out at room temperature and inside a glove box, under controlled atmosphere, to avoid dust contamination.

Erosion process in selected set-up is outlined in Fig. 1. After cell immersion in DW water, compacted clay pellet is hydrated and clay swelling is favoured but, due to confinement, free swelling is not allowed. The clay is expected to extrude through the pores of the filters, which resemble the rock micro-fractures. Eroded particles can be released to the contact water, without any additional force. By analysing the liquid phase, we measure the fraction of particles eroded and released to the liquid phase.

According to previous studies, selected filters have sufficient pore size (100 µm) not interfering in the erosion process. For example, in Grissinger (1966) measured clay erodibility under flow conditions with a filter with pores of 5 µm diameter. Equivalent colloid releases were measured from compacted bentonite with 2, 10 and 100 µm pore sizes (Seher et al., 2009). For Na-clays, no filter effects were observed on erosion by Birgersson et al. (2009), until reducing pore sizes down to 0.5 µm and for Ca-clays for sizes of 100 µm, when little to no erosion was measured.

To quantify clay erosion and to relate erosion values to the physico-chemical and structural properties of the clays, the aqueous phase was periodically sampled (2 mL) for two years, to analyse the particles eroded from the compacted clays.

Photon Correlation Spectrometry (PCS) technique (Holthoff et al., 1996) was selected to evaluate the concentration of eroded particles and their average hydrodynamic diameter. PCS measurements were carried out with a Zetasizer NanoS Malvern equipment with a He-Ne laser source of $\lambda = 633$ nm and detection at 173°, which features allow measuring particles from 2 nm to 3 µm at particle concentrations higher than 0.5 mg L^{-1}. The errors of size measurements are obtained by the standard deviation of at least five measurements.

Particle mass and concentration were determined with calibration curves of PCS count-rate *vs*. concentration (Ledin et al., 1993). Calibration curves were obtained with laboratory prepared bentonite colloid suspensions, of known size and concentration, obtained in deionised water by centrifuging the different bentonites at 600 g during 20 min. The colloid concentration was determined by gravimetric measurements.

The mass background was determined immersing the erosion cell components in 200 mL of deionised water and by periodically analysing the water during 420 days. Considering the cell components background and the equipment resolution, detection limit under experimental conditions is around 1 mg.

Chemical analyses were carried out, at the end of the experiment, on the final electrolytes. These studies aim to analyse chemical changes (major and trace elements) promoted by the presence of bentonite, in relation to erosion masses. Major and trace cations were analysed by inductively coupled plasma atomic emission spectrometer (Varian 735ES, AA240 FS). Sodium and potassium were determined by atomic absorption spectrometry using a Agilent AA 240 FS spectrometer. Anions were analysed by ion chromatography (DIONEX ICS-2000). Geochemical calculations were carried out with the code Geochemist's Workbench® (v. 8.0).

At the end of the experiment, the clay fraction eventually retained in the filter pores (100 µm pore size) was analysed to evaluate if clay clogging occurred during the experiment. The filters were weighted at the end of the experiment and after an acid treatment (with HCl 1 M) to facilitate clay removal. The remaining mass in the filters was maximum with NANOCOR® clay (0.035 g per filter) and lower than 1.5% of the initial mass in any case, being far from the 0.9 g that would fit in a filter (estimated considering filter dimensions and a clay density of 2.7 g cm^{-3}). This fully discard clay clogging in filter pores. In other erosion experiments, carried out in artificial fractures, the clay fraction extruded in the fracture is sometimes accounted for as eroded (Missana, 2016; Schatz et al., 2016). In our case, the masses extracted from the filters may be affected by filter dissolution, due to the strong acid treatment. Therefore, in this study, (only) the fraction of particles detached and released to the liquid phase is consider as eroded.

As mentioned, eroded masses obtained here from compacted and confined clays were compared with those measured in free-dispersion

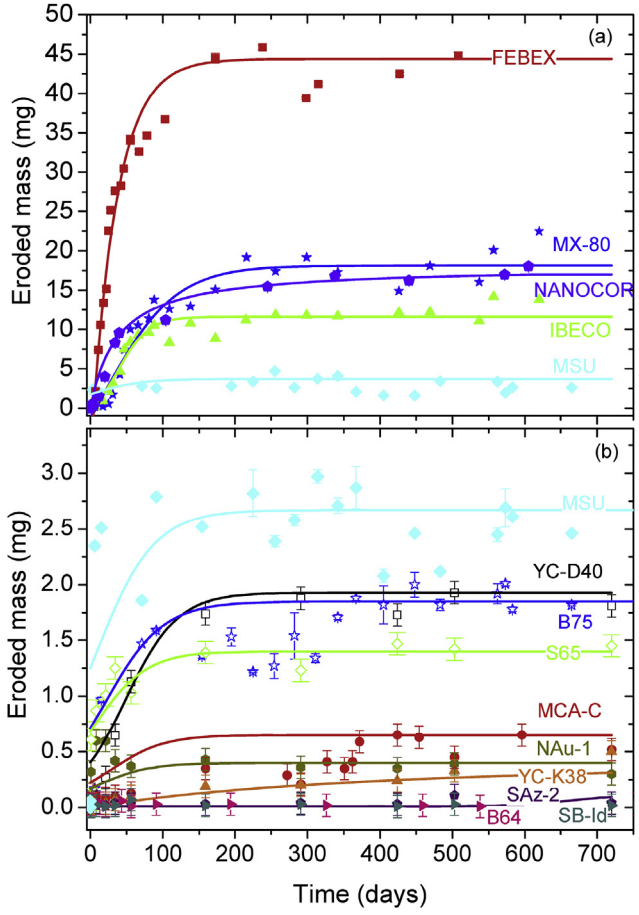

Fig. 2. Eroded mass measured, as a function of time, from different raw bentonites compacted at 1.65 g cm^{-3} and immersed in deionised water during 600–700 days. (a) Clays showing appreciable eroded masses; (b) Clays with eroded masses lower than 5 mg. The lines are included to guide the eye and the label of each clay is indicated.

experiments, where maximum colloid formation was determined after suspending 1 gram of different clays in 1 litre of deionised water (DW), to maximize their dispersion. After centrifuging, the supernatant was collected and the mass, surface charge and particle size were determined. The mass of dispersed colloids was considered the first important parameter to assess clay erodibility (Missana et al., Submitted).

3. Results and discussion

Fig. 2 presents the eroded mass (in mg) measured, as a function of time, in 200 mL of electrolyte in contact to the different raw bentonites compacted at 1.65 g cm^{-3} and adequately confined. The initial electrolyte was deionised water (DW). Lines were included to guide the eye.

Fig. 2a shows those experiments where measured eroded masses were appreciable (mass > 5 mg). The highest values were measured for FEBEX clay (40 mg), followed by MX-80, Nanocor® and IBECO clays, which are clays with exchangeable Na^+ content higher than a 20% of the cation exchange capacity (CEC) and a smectite content (Sm.) ≥ 80 wt % (Table 1). In Fig. 2b, the eroded mass (mg) measured for those bentonites showing limited (mass 1–2 mg: MSU, YC-D40 and Rokle B75) or negligible erosion (mass < 1 mg: MCA-C, NAu-1, YC-K38, SAz-2, B64, SBId-1) are presented. Eroded mass was determined by PCS analyses by using calibration curves obtained with laboratory prepared colloids of known concentrations. Equipment resolution limits precise quantification of masses lower than 1 mg, under experimental conditions.

All clays exhibited a similar behaviour in the sense that eroded mass initially increased with time but, after about 100 days, achieved an equilibrium, as previously observed (Albarran et al., 2014; Alonso et al., 2007). However, the magnitude of erosion was significantly different amongst the different clays. After equilibrium was reached, the average of last measured values was taken as eroded mass. Erosion masses eroded from compacted clay were low and, even considering the maximum values measured for FEBEX clay, obtained mass (40 mg) represented an erosion of only 1% of the mass initially installed (4–4.5 g), and the percentage of eroded mass dropped to a 0.06% for the MSU clay.

Table 4 summarizes the masses eroded (in mg) from all studied bentonites. In this table, values were presented in different units (mg and ppm) and normalised to the area available for transport (in kg/m^2, considering the surface area of two filters: $3.54{\cdot}10^{-4}$ m^2) to facilitate the comparison with other experiments.

In Table 4, the average hydrodynamic diameter measured by PCS for eroded particles was also included. When appreciable erosion was measured, the eroded particles had an average diameter of around 300–500 nm, values that are by definition in the colloid range (< 1 μm). The smallest diameters were measured for Nanocor®, the clay with higher smectite content and higher Na^+ content at interlayer sites, in agreement to previous observations, under free-dispersed conditions, where the higher the Na^+ content was the smaller the particles were, (Missana et al., Submitted). The particle size conditions transport and stability (Missana et al., 2018a; Albarran et al., 2013).

Table 4
Maximum masses eroded from bentonites compacted at 1.65 g cm^{-3} in deionised water, and average particle diameters measured by PCS. Eroded masses are presented in different units to consider the final water volumes (ppm) and surface available for transport (kg/m^2), calculated considering $3.54{\cdot}10^{-4}$ m^2 (two filters surface area).

Clay	Eroded mass (mg)	Eroded mass (ppm)	Eroded mass (kg/m^2)	Average particle diameter (nm)
NANOCOR®	24.8 ± 4	146 ± 24	$(7.0 \pm 1.1){\cdot}10^{-2}$	248 ± 31
MSU	2.67 ± 1	17.2 ± 6.4	$(7.6 \pm 2.8){\cdot}10^{-3}$	299 ± 88
FEBEX	40 ± 5	268 ± 30	$(1.3 \pm 0.2){\cdot}10^{-1}$	333.5 ± 42
MX-80	18.29 ± 0.5	120 ± 3.2	$(5.2 \pm 0.1){\cdot}10^{-2}$	286 ± 30
MILOS-IBECO	14 ± 1	92 ± 7	$(4.0 \pm 0.3){\cdot}10^{-2}$	386 ± 50
Rokle S65 fully activated	1.45 ± 0.21	8 ± 1	$(4.1 \pm 0.6){\cdot}10^{-3}$	468 ± 50
Rokle B75 (part. Activated)	1.9 ± 0.5	11 ± 3	$(5.4 \pm 1.4){\cdot}10^{-3}$	286 ± 80
YC-D40	1.8 ± 0.1	10 ± 0.6	$(5 \pm 0.3){\cdot}10^{-3}$	352 ± 22
YC-K38	0.3 ± 0.1	1.7 ± 0.6	$(8.5 \pm 2.8){\cdot}10^{-4}$	372.7 ± 71
SBId-1 (Beidellite)	0.02 ± 0.03	0.1 ± 0.2	$(5.7 \pm 0.8){\cdot}10^{-4}$	1625 ± 138
NAu-1 (Nontronite)	0.4 ± 0.22	2 ± 1	$(1.1 \pm 0.6){\cdot}10^{-3}$	1260 ± 300
SAz-2 - Cheto	0.05 ± 0.04	0.3 ± 0.2	$(1.4 \pm 1.1){\cdot}10^{-4}$	821.8 ± 290
MCA-C (Saponite)	0.65 ± 0.34	3.6 ± 1.9	$(1.8 \pm 0.9){\cdot}10^{-3}$	995 ± 50
B64 (Saponite)	0.03 ± 0.02	0.2 ± 0.1	$(8.5 \pm 5.7){\cdot}10^{-5}$	907 ± 115

The obtained masses were compared to those obtained under dispersed conditions (Missana et al., Submitted), where potential erodibility is maximised. At first sight, clearly lower erosion masses were measured under compacted and confined conditions (Table 4). Under free dispersed conditions, maximum erosion was measured for Na-nocor® clay (735 ppm), which is by far higher than the value measured here (24.8 mg or 146 ppm). And moreover, Nanocor®, despite of being the clay with higher smectite and Na^+ content, it was not the clay that shows the highest erosion under compacted conditions (Table 3), being surpassed by FEBEX clay (40 mg or 238 ppm).

Amongst the clays that undergo erosion, eroded masses are low, which prevent obtaining strong dependencies. The variability of values may be attributed to the raw nature of studied clays, which are not pure smectites, and which have (oxy)hydroxides and other accessory minerals in their composition, and the erosion behaviour of natural bentonites could deviate from the pure smectite behaviour (Milodowski et al., 2016), as it has been already observed for other properties like cation exchange (Meunier et al., 1992), or swelling capacity (Montes-H et al., 2005). For example, Czech bentonites (B75 and S65) have appreciable illite and kaolinite and also different Fe oxides (Fernández et al., 2017a), which may contribute to inhibit erosion, since they affect bentonite colloid stability (Mayordomo et al., 2014). The ability of Al and Fe oxides to reduce clay swelling and to promote clay flocculation has been observed (Goldberg and Glaubig, 1987) and being considered more efficient in Ca-dominated clays than on Na-clays. The relevance of minor minerals and (oxy)hydroxides present in the clay on erosion behaviour should be further analysed.

3.1. Role of smectite content and exchangeable cations

Fig. 3 presents the maximum masses eroded from the different raw bentonites, as a function of the smectite (Sm.) content. In this figure, the bentonites were plotted in three groups, according to their erosion, from lower to higher values: mass < 1 mg (black triangles), mass between 1 and 5 mg (red circles) and mass > 5 mg (blue squares).

Higher erosion was measured for clays with higher smectite content while the Ypresian clays, the with lower smectite content (Sm. < 30 wt %), showed erosion values lower than 2 mg.

Eroded masses from clays where appreciable erosion was measured showed rather good correlation with the clay smectite content, with the exception of Nanocor® clay, which has the highest smectite and Na^+ content (Table 2), but not the highest erosion.

In free dispersion studies, also carried out in deionised water, correlation between colloid mass released and smectite content was observed for Na- and mixed Na/Ca mixed clays (Missana et al., Submitted). The dependence here was much more abrupt and erosion dropped for clays with smectite content below a 90 wt%.

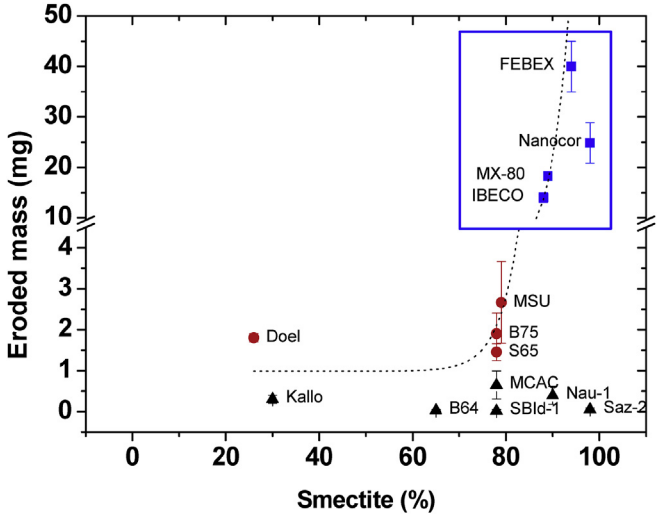

Fig. 3. Eroded mass measured in deionised water from different raw bentonites compacted at 1.65 g/cm^3, as a function of the smectite content. Dashed line was included to guide the eye.

Excluding Ypressian clays (YC-Doel-40 and YC-Kallo-38), for their low smectite content, all smectites that showed negligible erosion (nontronite NAu-1, beidellite SBId-1, SAz-2 "Cheto" clay and MCA-C and B64 saponites) have very low Na content in the exchange complex (Na^+ < 10% and Ca^{2+} + Mg^{2+} > 90%); so that they can be defined as *Ca/Mg clays*. This indicated that high content of bivalent cations (Ca^{2+} + Mg^{2+} > 90%) was a dominant factor affecting erosion, in this case inhibiting it (Fig. 3a). In fact, it is considered that smectites with more than 90% of Ca do not form sols (Birgersson et al., 2009), and low erodibility of Ca-dominated soils is usually reported (Grissinger, 1966).

The rest of the clays have smectite content from 78% (Rokle-S65 and Rokle-B75) up to 98% (Nanocor®) and a wide range of Na^+ content: mixed Na/Ca-clays with Na^+ content slightly higher than 25% (FEBEX or IBECO) up to Na-clays with Na^+ content higher than a 90% of the cation exchange capacity higher than a 90% (MSU and Nanocor®). Nanocor® and MSU clays have higher Na^+ content but they are not the most eroded clays, being erosion mass higher for FEBEX with a Na^+ content lower than 30%. Therefore, eroded masses were not correlated to the Na^+ content.

This independence of masses eroded from compacted clays of the clay Na content was striking at first sight, because it is well-known that the presence of Na^+ in the interlayer (approximately above 20%) causes disaggregation of clay platelets and the formation of smaller tactoids (Banin and Lahav, 1968), and that the Na^+ content in the exchange complex affects clays dispersion (Bell and Stenius, 1980). In free-dispersion experiments, higher colloid masses were generated from laboratory exchanged Na-homoionic clays, but similar quantity of colloids were generated from raw mixed Na/Ca clays (Kaufhold and Dohrmann, 2008; Missana et al., Submitted).

Previous experiments carried out with compacted clays showed that erosion mass from laboratory prepared Na-homoionic FEBEX was higher than from raw FEBEX bentonite, and almost zero from Ca-homoionic FEBEX, both under stagnant (Albarran et al., 2014) or flow conditions (Missana et al., 2011).

The fact that masses eroded from Na-homoionic clay samples verified dependency on the Na content, not clearly observed in raw clays, suggested that accessory minerals or oxides present in the clay, the salt inventory and/or properties related to compaction are playing an important role. In fact, experimental conditions are transient and electrolyte and porewater concentrations evolved with time.

One of the characteristics of smectite clays is its swelling capacity, and thus, a relationship between erosion mass and swelling pressure was not discarded. Swelling pressure reported for FEBEX bentonite at 1.65 g cm^{-3} dry density is 5 MPa (Huertas et al., 2000) and that for MX-80 or IBECO clays, against deionised water, is around 12 MPa, (Karnland, 2010). The fact that swelling pressures are not available in the open literature for all the studied clays prevents an assessment. Swelling ability of smectites is affected by the water uptake and their salinity, by the exchangeable cations (Norrish, 1954) and by the charge distribution.

3.2. Role of layer charge and charge distribution

Fig. 4 shows the mass eroded from the different bentonites, normalised to the clay smectite content (%), as a function of the clay tetrahedral charge per half unit cell (*e*/h.u.c), expressed in absolute values. In the figure, the clays whose low erodibility was already explained by their low smectite content (Sm. < 70 wt %) or by cation exchange capacity dominated by divalent cations (Ca^{2+} + Mg^{2+} > 90%) are plotted with open symbols.

Eroded mass decreased as the tetrahedral charge increased (in

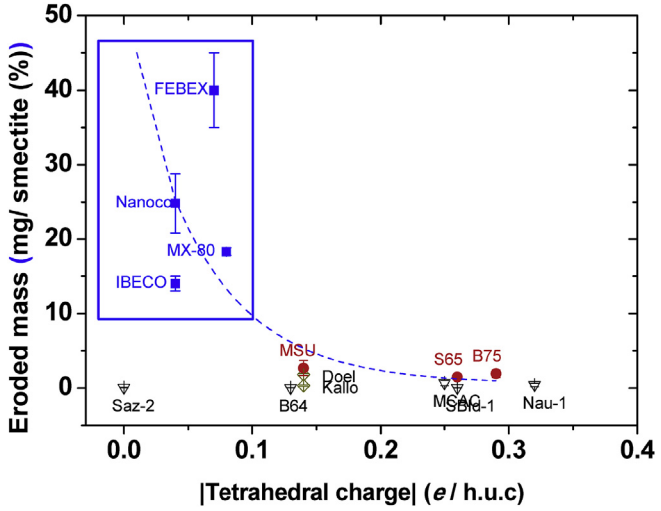

Fig. 4. Mass eroded from different raw bentonites normalised to clay smectite content (mg/% Sm) as a function of clay tetrahedral charge (in absolute values (*e*/h.u.c): (■) Clays with eroded mass > 5 mg; (●) Clays with eroded mass 1–5 mg. (◇) Clays with smectite content < 30% (YC-Doel40 and YC-Kallo38); (▽) Clays with (Ca^{2+} + Mg^{2+}) > 90% (SBId-1, NAu-1, SAz-2, MCA-C and B64). Dashed line was included to guide the eye).

absolute value), with the only exception of SAz-2 clay, which have null tetrahedral charge but negligible erosion, explained by its Ca-nature, a dominant factor hindering erosion. All clays that suffered erosion have low tetrahedral charge (τ), between 0 and 0.1 *e*/h.u.c, where *e* is the electron charge, while those clays whose tetrahedral charge is higher than 0.1 *e*/h.u.c exhibited limited (MSU, S65 and B75) or negligible erosion (Ca/Mg-clays: beidellite, nontronite and saponite). The low erosion of saponites has been attributed to their tri-octahedral nature (Mantovani et al., 2009).

The closer the charges are located to the surface, the stronger the repulsion between clay basal surfaces should be, providing favourable detachment conditions. But on the other hand, more surface localised charges should enhance the interactions with interlayer cations, which could inhibit swelling. In principle, an increase of tetrahedral charge is expected to strengthen the interactions between TOT layers, lowering particle detachment (Hetzel and Doner, 1993). Under compacted conditions, the interlayer space is reduced and TOT interactions are additionally favoured, affecting the electrical interactions of charge layers (overlapping of electrical double layers). An increase of TOT interactions is expected to limit detachment.

Low tetrahedral charge also leads to smaller particles and particle size increases as tetrahedral charge increases (Missana et al., Submitted), and this is verified for all clay groups (Tables 2 and 4).

3.3. Role of clay/water interactions and chemical equilibrium

Results have shown that the low erodibility measured for most clays can be attributed to their low smectite content, high content of divalent cations and high tetrahedral charge, but still, it is not clear why the clay with highest smectite and Na^+ content, low tetrahedral charge is not the clay which exhibits highest erosion.

Under compacted and confined conditions, the solid to liquid ratio is higher than in free dispersed experiments (20 g L^{-1} compared to 1 g L^{-1}), so that clay/water interactions may be enhanced.

The water chemistry was analysed at the end of the experiments. Table 5 presents the concentration of major ions, measured in waters in equilibrium with all studied clays, and the pH and conductivity measured at the end of the experiments. In all cases, initial water is deionised, but measured electrical conductivities at the end of the experiment increased, indicating that dissolution of soluble salts present in the clay occurred (Table 3).

According to the major anions measured, dissolution of halite (NaCl), gypsum ($CaSO_4{\cdot}2H_2O$) and also calcite ($CaCO_3$) occurred, the Cl and SO_4 concentrations being in most cases in agreement with the anion inventory present in the clays, especially with calcite (Table 3). The clay with higher anion content in the salt inventory was Nanocor®, probably coming from the industrial treatment used to homoionise the clay.

If we look to the concentration of major cations (Na^+, Ca^{2+} and Mg^{2+}) measured in the water at equilibrium, (initially deionised water), values suggested that cation exchange processes took place, because Na concentrations are higher than expected assuming only halite dissolution, and Ca concentrations in solutions are lower. This means that the initial content of cations in exchangeable positions is varying. (Dohrmann et al., 2013) observed that the type of dominant interlayer cation initially present is less important than the surrounding water. An increase of bivalent cations in exchangeable positions is expected to hinder erosion.

The ionic strength was calculated with measured cation and anion concentrations, and obtained values are confirmed by measured conductivities (Table 5). Fig. 5 presents the eroded mass obtained from the different bentonites as a function of the ionic strength at equilibrium. In this figure, the clays whose low erodibility was explained by their low smectite content (Sm. < 60 wt%), by their high content of divalent cations (Ca^{2+} + Mg^{2+} > 90%) and by their high tetrahedral charge (|τ| > 0.1 *e*/h.u.c) are plotted with open symbols.

The ionic strength values measured in the water at equilibrium for Ca/Mg clays were generally low, while the highest ionic strength (~10^{-2} M) were measured for the Na-clays (Nanocor® and MSU), values explained by dissolution of soluble salts (Cl^- and SO_4^{2-}) in their inventory. The rest of the clays have values between $2{\cdot}10^{-3}$ M and $9{\cdot}10^{-3}$ M. The lower ionic strength measured for FEBEX, clay compared to that of IBECO, MX-80 and, especially Nanocor® clay, may explain its higher erosion.

Results obtained from several erosion experiments carried out under different experimental conditions led to the conclusion that a salinity higher than 1–$2{\cdot}10^{-2}$ M (in Na) inhibits the erosion process (Missana, 2016; Schatz et al., 2016). According to (Birgersson et al., 2009), montmorillonites do not suffer erosion when the external ionic strength is higher than $4{\cdot}10^{-3}$ M, for Na-bentonites, or higher than $2.5{\cdot}10^{-3}$ M for mixed Na/Ca montmorillonites (Ca^{2+} > 20%). Critical coagulation concentrations against Na and Ca electrolytes are published in Missana et al. (2018a).

Ionic strengths measured at equilibrium approach the values which are considered to limit, and could partially explain the lower erosion measured (lower than 1% of the initial mass installed) under compacted conditions, in comparison free dispersed conditions (Missana et al., Submitted). In addition, the reduced erosion measured for the clay with highest smectite and Na^+ content can be related to its highest ionic strength. In fact, its inherent characteristics, high smectite content and Na-nature had probably favoured appreciable erosion, not fully inhibited by water chemistry.

These chemical effects which inhibit erosion would be enhanced at a higher solid to liquid ratio. In natural groundwaters with relatively low ionic strengths, low clay colloid concentration (< 1 mg L^{-1}) was found (Degueldre and Benedicto, 2012; Degueldre and Laaksoharju, 2014; Degueldre et al., 1989a, 1989b, 1996), and even lower in groundwaters with high ionic strength groundwater (Degueldre and Laaksoharju, 2014; Iwatsuki et al., 2017).

In a high-level radioactive waste (HLRW) repository, geochemical evolution of bentonite is expected at the long term due to the water income (Wallis et al., 2016) and heating (Fernández and Villar, 2010; Fernández et al., 2017b). For example, in the FEBEX experiment (Grimsel Test Site, Switzerland) (Huertas et al., 2000), where a bentonite barrier simulating a HLWR was installed at a real scale in a granite area with hydraulic conductivities in the range of 10^{-11} m/s, it was

Table 5
Chemical characteristics of water equilibrated with clay erosion cells during 600–700 days.

Clay	pH_{FIN}	$Cond_{FIN}$ µS/cm^2	Ca^{2+} (M)	Mg^{2+} (M)	Na^{+} (M)	K^{+} (M)	HCO_3^{-} (M)	SO_4^{2-} (M)	Cl^{-} (M)	Ionic strength (M)
NANOCOR®	7.42	673	$1.0\cdot10^{-5}$	$1.4\cdot10^{-4}$	$6.1\cdot10^{-3}$	$2.8\cdot10^{-5}$	$9.8\cdot10^{-4}$	$2.3\cdot10^{-3}$	$7.1\cdot10^{-4}$	$8.6\cdot10^{-3}$
MSU	9.88	719	$1.0\cdot10^{-5}$	$8.6\cdot10^{-6}$	$8.3\cdot10^{-3}$	$5.9\cdot10^{-5}$	$5.1\cdot10^{-3}$	$4.8\cdot10^{-4}$	$3.9\cdot10^{-4}$	$3.6\cdot10^{-3}$
FEBEX	8.20	190	$1.2\cdot10^{-5}$	$9.1\cdot10^{-5}$	$1.9\cdot10^{-3}$	$2.6\cdot10^{-5}$	$1.2\cdot10^{-3}$	$2.3\cdot10^{-4}$	$4.2\cdot10^{-4}$	$1.4\cdot10^{-3}$
MX-80	8.86	364	$1.4\cdot10^{-5}$	$8.6\cdot10^{-5}$	$3.8\cdot10^{-3}$	$3.3\cdot10^{-5}$	$2.4\cdot10^{-3}$	$7.0\cdot10^{-4}$	$1.0\cdot10^{-4}$	$2.8\cdot10^{-3}$
MILOS-IBECO	9.30	286	$2.1\cdot10^{-5}$	$4.5\cdot10^{-5}$	$2.7\cdot10^{-3}$	$5.1\cdot10^{-5}$	$1.8\cdot10^{-3}$	$3.3\cdot10^{-4}$	$1.4\cdot10^{-4}$	$1.9\cdot10^{-3}$
Rokle S65 (fully activated)	9.75	600	$7.7\cdot10^{-6}$	$1.3\cdot10^{-5}$	$6.1\cdot10^{-3}$	$6.7\cdot10^{-5}$	$4.8\cdot10^{-3}$	$2.3\cdot10^{-5}$	$2.5\cdot10^{-5}$	$6.5\cdot10^{-3}$
Rokle B75 (part. activated)	9.32	393	$2.0\cdot10^{-5}$	$2.3\cdot10^{-5}$	$5.2\cdot10^{-3}$	$1.5\cdot10^{-4}$	$4.7\cdot10^{-3}$	$4.0\cdot10^{-5}$	$1.7\cdot10^{-4}$	$1.9\cdot10^{-3}$
YC-D40	9.20	437	$3.5\cdot10^{-5}$	$1.4\cdot10^{-5}$	$4.0\cdot10^{-3}$	$2.1\cdot10^{-4}$	$2.6\cdot10^{-3}$	$1.4\cdot10^{-4}$	$1.0\cdot10^{-3}$	$1.3\cdot10^{-3}$
YC-K38	8.64	395	$1.3\cdot10^{-5}$	$8.6\cdot10^{-6}$	$3.6\cdot10^{-3}$	$1.7\cdot10^{-4}$	$2.0\cdot10^{-3}$	$6.2\cdot10^{-4}$	$3.4\cdot10^{-4}$	$1.1\cdot10^{-3}$
SBId-1 (beidellite)	5.00	42	$1.6\cdot10^{-5}$	$1.1\cdot10^{-5}$	$5.2\cdot10^{-5}$	$7.9\cdot10^{-5}$	$1.5\cdot10^{-3}$	$9.2\cdot10^{-6}$	$1.1\cdot10^{-4}$	$0.6\cdot10^{-5}$
NAu-1 (nontronite)	5.63	154	$6.7\cdot10^{-5}$	$4.5\cdot10^{-5}$	$9.6\cdot10^{-4}$	$6.4\cdot10^{-5}$	$1.2\cdot10^{-3}$	$2.2\cdot10^{-5}$	$9.9\cdot10^{-4}$	$4.7\cdot10^{-4}$
SAz-2 - Cheto	5.87	35	$5.2\cdot10^{-5}$	$1.2\cdot10^{-5}$	$6.1\cdot10^{-5}$	$2.1\cdot10^{-5}$	$7.4\cdot10^{-4}$	$2.0\cdot10^{-6}$	$1.1\cdot10^{-5}$	$2.8\cdot10^{-4}$
MCA-C (saponite)	7.84	79	$2.0\cdot10^{-5}$	$3.6\cdot10^{-5}$	$6.1\cdot10^{-4}$	$4.3\cdot10^{-5}$	$5.7\cdot10^{-4}$	$2.6\cdot10^{-5}$	$8.7\cdot10^{-5}$	$4.3\cdot10^{-4}$
B64 (saponite)	8.11	97	$1.4\cdot10^{-4}$	$3.2\cdot10^{-4}$	$3.9\cdot10^{-5}$	$2.3\cdot10^{-5}$	$8.5\cdot10^{-4}$	$6.2\cdot10^{-6}$	$1.4\cdot10^{-5}$	$1.4\cdot10^{-3}$

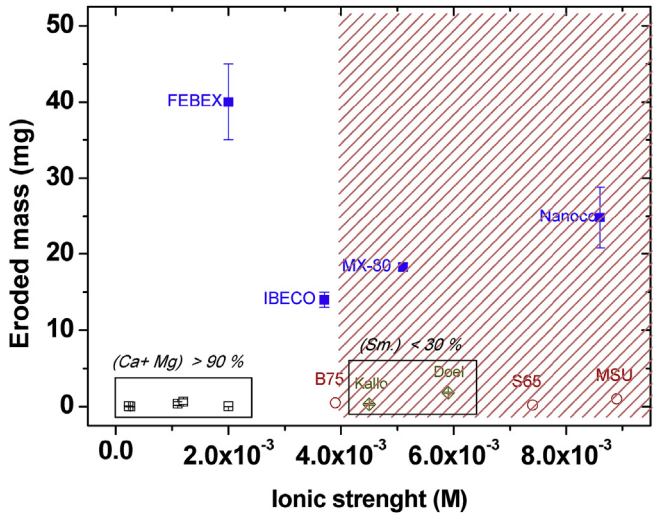

Fig. 5. Eroded mass measured in deionised water from different raw bentonites compacted at 1.65 g cm^{-3}, in relation to the ionic strength of the contact water at equilibrium. (■) Clays with eroded mass > 5 mg; (◇) Clays with smectite content < 30% (YC-Doel40 and YC-Kallo38); (▽) Clays with (Ca + Mg) > 90% (SBId-1, NAu-1, SAz-2, MCA-C and B64). (○) Clays with tetrahedral charge $|\tau|$ < 0.1 *e*/h.u.c.

found that, in the surrounding of the bentonite barrier, the groundwater chemistry changed from $CaHCO_3$ type to NaCl type (Buil et al., 2010). Increased ionic strengths are expected to inhibit erosion and colloid formation. In fact, at the FEBEX site, where groundwater chemical conditions where in principle favourable for colloid formation and stability, very little colloid concentrations (< 1 ppm) where measured (Missana et al., 2018b). Our results showed that, under repository conditions, clay/water interactions and chemical equilibrium will determine erosion behaviour of *a priori* erodible clays over their initial physico-chemical and structural characteristics.

4. Conclusions

The erosion behaviour of fourteen different natural bentonites, representative of relevant clay minerals form the smectite group, was analysed under compacted and confined conditions, characteristics of a bentonite barrier in a high level radioactive waste (HLRW), in deionised water, to account for favourable chemical conditions for erosion. Results were analysed in relation to the main physicochemical and structural characteristics of the clays and compared with results obtained under free-dispersed conditions.

The masses eroded measured under compacted and confined conditions and subjected to favourable chemical conditions (low ionic strength water in absence of divalent cations: deionised water) were in all cases very low. At maximum, eroded mass measured corresponds to a 1% of the initial mass installed. Obtained values are by far lower than those obtained under free-dispersed conditions, indicating that processes related to the compacted and confined conditions were limiting erosion. When appreciable erosion was measured, the average diameter of the eroded particles was around 300–500 nm, values that are by definition, in the colloid range (< 1 µm), what would affect their stability and transport behaviour.

Negligible erosion was measured from Ca/Mg-clays ($Ca^{2+} + Mg^{2+}$ > 90%), independently of their smectite content or charge distribution, indicating that high content of divalent cations in exchangeable positions is a dominant aspect affecting smectite erosion, in this case inhibiting it.

All clays which showed appreciable erosion have smectite content higher than 70 wt%. In addition, all erodible clays have tetrahedral charge lower than 0.1 *e*/h.u.c (in absolute value). Eroded masses decreased as tetrahedral charge (in absolute value) increases, because of clay layers interactions are strengthened, limiting detachment. However, eroded masses were not straightforward related to the main exchangeable cation, in contrast to that observed under free dispersed conditions.

The chemical analyses carried out at equilibrium revealed salt dissolution and cation exchange processes took place. Ionic strengths measured at equilibrium partially explained the limited erosion measured under compacted conditions, in comparison free dispersed conditions. In particular, the ionic strength of water in contact with studied Na-clays was higher, in agreement to the higher concentration of soluble salts in their inventory. This pointed out that, under repository conditions, where solid to liquid ratio is high, the clays salt inventory and clay/water interactions may play a very relevant role on erosion despite the structural characteristics of the clays.

Acknowledgments

The research leading to these results was mainly funded by the EU 7th Framework Programme (FP7/2007-2011) under the grant agreement N° 295487 (BELBAR, Bentonite Erosion: effects on the Long-term performance of the engineered Barrier and Radionuclide Transport) and by the MIRAME Project (CTM2014-60482-P) supported by the Spanish Ministry of Economy and Competiveness. The Chemistry Division of CIEMAT (Madrid, Spain) is greatly acknowledged for the chemical analyses.

References

Albarran, N., Missana, T., Alonso, U., Garcia-Gutierrez, M., Lopez, T., 2013. Analysis of latex, gold and smectite colloid transport and retention in artificial fractures in crystalline rock. Colloid. Surface a. Physicochem. Eng. Aspect. 435, 115–126.

Albarran, N., Degueldre, C., Missana, T., Alonso, U., García-Gutiérrez, M., López, T., 2014. Size distribution analysis of colloid generated from compacted bentonite in low ionic strength aqueous solutions. Appl. Clay Sci. 95, 284–293.

Alonso, U., Missana, T., Garcia-Gutierrez, M., 2007. Experimental approach to study the colloid generation from the bentonite barrier to quantify the source term and to assess its relevance on the radionuclide migration. Scien. Basis Nucl. Waste Manag. XXX MRS 985, 605–610.

Baik, M.-H., Cho, W.-J., Hahn, P.-S., 2007. Erosion of bentonite particles at the interface of a compacted bentonite and a fractured granite. Eng. Geol. 91, 229–239.

Banin, A., Lahav, N., 1968. Particle size and optical properties of montmorillonite in suspension. Isr. J. Chem. 6, 235–250.

Bell, J.C.L., Stenius, P., 1980. The influence of cations on particle interactions and particle release from aqueous bentonite gels. Powder Technol. 26, 17–27.

Bessho, K., Degueldre, C., 2009. Generation and sedimentation of colloidal bentonite particles in water. Appl. Clay Sci. 43, 253–259.

Birgersson, M., Hedstrom, M., Karnland, O., 2011. Sol formation ability of Ca/Na-montmorillonite at low ionic strength. Phys. Chem. Earth 36, 1572–1579.

Birgersson, M., Börgesson, L., Hedström, M., Karnland, O., Nilsson, U., 2009. Bentonite Erosion. SKB technical report, TR 09-34 (2009). .

Bradbury, M.H., Baeyens, B., 2009. Experimental and modelling studies on the pH buffering of MX-80 bentonite porewater. Appl. Geochem. 24, 419–425.

Bütak, T., 2005. Clay minerals, Ca/Mg ratio and Fe-Al-oxides in relation to structural stability, hydraulic conductivity and soil erosion in southeastern Turkey. Turk. J. Agric. For. 29, 29–37.

Buil, B., Gomez, P., Peña, J., Garralon, A., Turrero, M.J., Escribano, A., Sanchez, L., Duran, J.M., 2010. Modelling of bentonite-granite solutes transfer from an in-situ full-scale experiment to simulate a deep geological repository (Grimsel Test Site, Switzerland). Appl. Geochem. 25, 1797–1804.

Chapman, N., 2006. Geological disposal of radioactive wastes – concept, status and trends. J. Iber. Geol. 32, 7–14.

Cuevas, J., Pelayo, M., Rivas, P., Leguey, S., 1993. Characterization of Mg-clays from the Neogene of the Madrid Basin and their potential as backfilling and sealing material in high level radioactive waste disposal. Appl. Clay Sci. 7, 383–406.

Degueldre, C., Benedicto, A., 2012. Colloid generation during water flow transients. Appl. Geochem. 27, 1220–1225.

Degueldre, C., Laaksoharju, M., 2014. Ground water colloid properties from the Bangombe system. Appl. Geochem. 45, 130–143.

Degueldre, C., Pfeiffer, H.R., Alexander, W., Wernli, B., Bruetsch, R., 1996. Colloid properties in granitic groundwater systems. I: sampling and characterization. Appl. Geochem. 11, 677–695.

Degueldre, C., Baeyens, B., Goerlich, W., Riga, J., Verbsit, J., Stadelmann, P., 1989a. Colloids in water from a subsurface fracture in granitic trock, Grimsel Test Site, Switzerland. Geochim. Cosmochim. Acta 53, 603–610.

Degueldre, C., Longworth, G., Moulin, V., Vilks, P., Ross, C., Bidoglio, G., Cremers, A., Kim, J., Pieri, J., Ramsay, J., Salbu, B., Vuorinen, U., 1989b. Grimsel Colloid Exercise: an International Intercomparison Exercise on the Sampling and Characterization of Groundwater Colloids. TM-36. Paul Scherrer Institute, Würenlingen and Villingen, Switzerland.

Dohrmann, R., Olsson, S., Kaufhold, S., Sellin, P., 2013. Mineralogical investigations of the first package of the alternative buffer material test – II. Exchangeable cation population rearrangement. Clay Miner. 48, 215–233.

Emmerich, K., Wolters, F., Kahr, G., Lagaly, G., 2009. Clay profiling: the classification of montmorillonites. Clay Clay Miner. 57, 104–114.

Fernández, A.M., Villar, M.V., 2010. Geochemical behaviour of a bentonite barrier in the laboratory after up to 8 years of heating and hydration. Appl. Geochem. 25, 809–824.

Fernández, A.M., Baeyens, B., Bradbury, M., Rivas, P., 2004. Analysis of porewater chemical composition of a Spanish compacted bentonite used in engineered barrier. Phys. Chem. Earth 29, 105–118.

Fernández, A.M., Missana, T., Alonso, U., Rey, J.J., Sánchez-Ledesma, D.M., Melón, A., Robredo, L.M., 2017a. Characterisation of Different Bentonites in the Context of BELBAR Project (Bentonite Erosion: Effects on the Long Term Performance of the Engineered Barrier and Radionuclide Transport) CIEMAT Report 100 Pp. Madrid (Spain).

Fernández, A.M., Sánchez-Ledesma, D.M., Melón, A., Robredo, L.M., Rey, J.J., Labajo, M., Clavero, M.A., Fernández, S., González, A.E., 2017b. Thermo-hydro-chemical (THC) Behaviour of a Spanish Bentonite after Dismantling of the FEBEX in Situ Test at the Grimsel Test Site. Nagra Report NTB 16-25. .

Gailhanou, H., Vieillard, P., Blanc, P., Lassin, A., Denoyel, R., Bloch, E., De Weireld, G., Gaboreau, S., Fialips, C.I., Made, B., Giffaut, E., 2017. Methodology for determining the thermodynamic properties of smectite hydration. Appl. Geochem. 82, 146–163.

Garcia-Garcia, S., Degueldre, C., Wold, S., Frick, S., 2009. Determining pseudo-equilibrium of montmorillonite colloids in generation and sedimentation experiments as a function of ionic strength, cationic form, and elevation. J. Colloid Interface Sci. 335, 54–61.

Goldberg, S., Glaubig, R.A., 1987. Effect of saturating cation, pH and aluminum and iron oxide on the flocculation of kaolinite and montmorillonite. Clay Clay Miner. 35, 220–227.

Grissinger, E.H., 1966. Resistance of selected clay systems to erosion by water. Water Resour. Res. 2, 131–138.

Guggenheim, S., Adams, J.M., Bain, D.C., Bergaya, F., Brigatti, M.F., Drits, V.A., Formoso, M.L.L., Galan, E., Kogure, T., Stanjek, H., 2006. Summary of recommendations of nomenclature committees relevant to clay mineralogy: report of the Association Internationale pour l'Etude des Argiles (AIPEA) Nomenclature Committee for 2006. Clay Miner. 4, 863–877.

Hetzel, F., Doner, H.E., 1993. Some colloidal properties of beidellite: comparison with low and high charge montmorillonites. Clay Clay Miner. 41.

Holthoff, H., Egelhaaf, S.U., Borkovec, M., Shurtenberger, P., Sticher, H., 1996. Coagulation rates of colloidal particles by simultaneous static and dynamic light scattering. Langmuir 12, 5541–5549. http://www.nanocor.com/.

Huertas, F., Fuentes-Santillana, J.L., Jullien, F., Rivas, P., Linares, J., Fariña, P., Ghoreychi, M., Jockwer, N., Kickmaier, W., Martínez, M.A., Samper, J., Alonso, E., Elorza, F.J., 2000. Full Scale Engineered Barriers Experiment for a Deep Geological Repository for High-level Radioactive Waste in Crystalline Host Rock. EC Final REPORT EUR 19147. EC Final REPORT EUR 19147. .

Iwatsuki, T., Munemoto, T., Kubota, M., Hayashida, K., Kato, T., 2017. Characterization of rare earth elements (REEs) associated with suspended particles in deep granitic groundwater and their post-closure behavior from a simulated underground facility. Appl. Geochem. 82, 134–145.

Jaynes, W.F., Bigham, J.M., 1987. Charge reduction, octahedral charge and lithium retention in heated Li-saturated smectite. Clay Clay Miner. 35, 440–448.

Kallay, N., Barouch, E., Matijevic, E., 1987. Diffusional detachment of colloidal particles from solid7solution interfaces. Adv. Colloid Interface Sci. 27, 1–42.

Karnland, O., 2010. Chemical and Mineralogical Characterization of the Bentonite Buffer for the Acceptance Control Procedure in a KBS-3 Repository. SKB Technical Report TR-10-60, Stockholm. .

Karnland, O., Birgersson, M., Hedstrom, M., 2011. Selectivity coefficient for Ca/Na ion exchange in highly compacted bentonite. Phys. Chem. Earth 36, 1554–1558.

Kastridis, I.D., Kacandes, G.H., Mposkos, E., 2003. The palygorskite and Mg-Fe smectite clay deposits of the Ventzia basin, western Macedonia, Greece. In: Eliopoulus (Ed.), Mineral Exploration and Sustainable Development. Millpress, Rotterdam, pp. 891–894.

Kaufhold, S., Dohrmann, R., 2008. Detachment of colloidal particles from bentonites in water. Appl. Clay Sci. 39, 50–59.

Kaufhold, S., Dohrmann, R., 2016. Distinguishing between more and less suitable bentonites for storage of high-level radioactive waste. Clay Miner. 51, 289–302.

Kaufhold, S., Kacandes, G., Chryssikos, G., Gionis, V., Ufer, K., Dohrmann, R. (In Prep). Geochemical and Mineralogical Characterization of Mg-fe Smectites from Macedonia.

Keeling, J.L., Raven, M.D., Gates, W.P., 2000. Geology and characterization of tow hydrotheral nontronites form weathered metamorphic rocks at the Uley graphite mine, south Australia. Clay Clay Miner. 48, 537–548.

Koch, D., 2002. Bentonites as a basic material for technical base liners and site encapsulation cut-off walls. Appl. Clay Sci. 21, 1–11.

Koch, D., 2008. European bentonites as alternatives to MX-80. Sci. Technol. Ser. 334, 23–30.

Konta, J., 1986. Textural variation and composition of bentonite derived from basaltic ash. Clay Clay Miner. 34, 257–265.

Ledin, A., Karlsson, S., Düker, A., Allard, B., 1993. Applicability of PCS for measurement of concentration and size distribution in natural waters. Anal. Chim. Acta 281, 421–428.

Liu, J., Neretnieks, I., 2006. Physical and Chemical Stability of the Bentonite Buffer. SKB Rapport R-06-103. Royal Institute of Technology, Stockholm (Sweden).

Liu, L., 2010. Permeability and expansibility of sodium bentonite in dilute solutions. Colloid. Surface a. Physicochem. Eng. Aspect. 358, 68–78.

Liu, L., Moreno, L., Neretnieks, I., 2009. A dynamic force balance model for colloidal expansion and its DLVO-based application. Langmuir 25, 679–687.

Luckham, P.F., Rossi, S., 1999. The colloidal and rheological properties of bentonite suspensions. Adv. Colloid Interface Sci. 82, 43–92.

Mantovani, M., Escudero, A., Alba, M.D., Becerro, A.I., 2009. Stability of phyllosilicates in Ca(OH)(2) solution: influence of layer nature, octahedral occupation, presence of tetrahedral Al and degree of crystallinity. Appl. Geochem. 24, 1251–1260.

Marcke, P.V., Laenen, B., 2005. The Ypresian Clays as Possible Host Rock for Radioactive Waste Disposal: an Evaluation. NIROND TR.2005-01 Report (Belgium). .

Mayordomo, N., Alonso, U., Missana, T., Benedicto, A., García-Gutiérrez, M., 2014. Addition of Al_2O_3 nanoparticles to bentonite: effects on surface charge and Cd sorption properties. In: Scientific Basis For Nuclear Waste Management XXXVII. Mat. Res. Symp. Proc. 1665. 978-1-60511-642-6, pp. 131–138.

Meunier, A., Beuafort, P.D., Lajudie, A., Petit, J.C., 1992. Heterogeneous reactions of dioctahedral smectites in illite-cmectite and kaolinite-smectite mixed-layers-Applications to clay materials for engineered barriers. Appl. Geochem. 7.

Milodowski, A.E., Norris, S., Alexander, W.R., 2016. Minimal alteration of montmorillonite following long-term interaction with natural alkaline groundwater: implications for geological disposal of radioactive waste. Appl. Geochem. 66, 184–197.

Missana, T., 2016. Evaluation of Experimental Results on Bentonite Erosion Deliverable D2.11 BELBAR Project. pp. 13.

Missana, T., Alonso, U., Turrero, M.J., 2003. Generation and stability of bentonite colloids at the bentonite/granite interface of a deep geological radioactive waste repository. J. Contam. Hydrol. 61, 17–31.

Missana, T., Alonso, U., García-Gutiérrez, M., Mingarro, M., 2008. Role of bentonite colloids on europium and plutonium migration in a granite fracture. Appl. Geochem. 23, 1484–1497.

Missana, T., Alonso, U., Fernández, A.M., García-Gutiérrez, M. (Submitted). Colloidal properties of different smectitic clays: significance for the bentonite barrier erosion and radionuclide transport in radioactive waste repositories. Appl. Geochem.

Missana, T., Alonso, U., Albarran, N., Garcia-Gutierrez, M., Cormenzana, J.-L., 2011. Analysis of colloids erosion from the bentonite barrier of a high level radioactive waste repository and implications in safety assessment. Phys. Chem. Earth 36,

1607–1615.
Missana, T., Alonso, U., Fernández, A.M., Lopez, T., García-Gutiérrez, M., 2018a. Analysis of stability behavior of colloids obtained from different raw bentonites for its implications on erosion processes in the frame of high-level waste repositories. Appl. Geochem. 92, 180–187.
Missana, T., Alonso, U., García-Gutiérrez, M., López, T., 2018b. Analysis of Bentonite Colloid Generation in the FEBEX Gallery at the Grimsel Test Site (Switzerland): Global Evaluation of the Experimental Data Obtained from 2006 to 2014. Colección Documentos CIEMAT, Madrid (Spain) ISBN-978-84-7834-.792-6.
Montes-H, G., Fritz, B., Clement, A., Michau, N., 2005. A simplified method to evaluate the swelling capacity evolution of a bentonite barrier related to geochemical transformations. Appl. Geochem. 20, 409–422.
Morgan, R.P.C., 2004. Soil Erosion and Conservation, third ed. Wiley-Blackwell.
Müller-Vonmoss, M., Kahr, G., 1983. Mineralogische Untersuchungen von Wyoming Bentonite MX-80 und Montigel. NTB 83-13, Nagra, Wettingen, Switzerland. .
Neretnieks, I., Liu, L., Moreno, L., 2009. Mechanisms and Models for Bentonite Erosion. SKB Technical Report TR-09-35. SKB, Sweden.
Nguyen, X.P., Cui, Y.J., Tanga, A.M., Li, X.L., Wouters, L., 2014. Physical and microstructural impacts on the hydro-mechanical behavior of Ypresian clays. Appl. Clay Sci. 102, 172–185.
Norrish, K., 1954. The swelling of montmorillonite. Discuss. Faraday Soc. 18, 120–134.
Odom, I.E., 1984. Smectite clay minerals: properties and uses. Phil. Trans. Roy. Soc. Lond. A 311, 287–299.
Pertsov, A.V., 2005. Quasi-spontaneous dispersion of solids. Colloid J. 67, 508–517.
Post, J.L., Cupp, I.D.L., Madsen, T., 1997. Beidellite and associated clays from the DeLamar Mine and Florida mountains area, Idaho. Clay Clay Miner. 45, 240–250.
Pusch, R., 1999. Clay colloid Formation and Release from MX80 Buffer. SKB Technical Report TR-99-31. SKB, Sweden.
Pusch, R., 2008. Geological Storage of Radioactive Waste. Springer.
Pusch, R., Karnland, O., Sanden, T., 1996. Final Report of Physical Test Program Concerning Spanish Clays (Saponites and Bentonites). ENRESA Report 02/96, (Spain). .
Ryan, J.N., Elimelech, M., 1996. Review: colloid mobilization and transport in groundwater. Colloid Surface A 107, 1–56.
Sabodina, M.N., Kalmykov, S.N., A.e.K.A., Z.E.V., S.Y.A., 2006. Behavior of Cs, Np(V), Pu (IV), and U(VI) in pore water of bentonite. Radiochemistry 48, 488–492.
Schaefer, T., Huber, F., Seher, H., Missana, T., Alonso, U., Kumke, M., Eidner, S., Claret, F., Enzmann, F., 2012. Nanoparticles and their influence on radionuclide mobility in deep geological formations. Appl. Geochem. 27, 390–403.
Schatz, T., Kanerva, N., Martikainen, J., Sane, P., Olin, M., Seppälä, A., Koskinen, K., 2013. Buffer Erosion in Dilute Groundwater. POSIVA Report 2012-44. Finland. .
Schatz, T., Eriksson, R., Hansen, E., Hedström, M., Missana, T., Alonso, U., Mayordomo, N., Fernández, A.M., Bouby, M., Heck, S., Geyer, F., 2016. WP2 Partners Final Report on Bentonite Erosion Deliverable D2.11 BELBAR Project. pp. 13.
Seher, H., Albarran, N., Hauser, W., Götz, R., Missana, T., Geckeis, H., Fanghänel, T., Schäfer, T., 2009. Colloid generation by erosion of compacted bentonite under different geochemical conditions. In: 4th FUNMIG Annual Workshop Proceedings, FZK Report FZKA 7461. FZK Karlsruhe, Germany, pp. 139–145.
Sellin, P., Leupin, O.X., 2013. The use of clays as an engineered barrier in radioactive-waste management: a review. Clay Clay Miner. 61, 477–498.
Sen, T.K., Khilar, K.C., 2006. Review on subsurface colloids and colloid-associated contaminant transport in saturated porous media. Adv. in Colloid. Interf. Sci. 119, 71–96.
Wallis, I., Idiart, A., Dohrmann, R., Post, V., 2016. Reactive transport modelling of groundwater-bentonite interaction: effects on exchangeable cations in an alternative buffer material in-situ test. Appl. Geochem. 73, 59–69.
Wersin, P., Kiczka, M., Koskinen, K., 2016. Porewater chemistry in compacted bentonite: application to the engineered buffer barrier at the Olkiluoto site. Appl. Geochem. 74, 165–175.